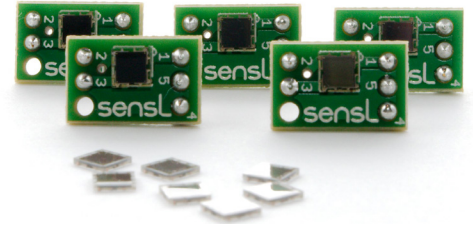


An Introduction to the Silicon Photomultiplier



The Silicon Photomultiplier (SiPM) is a sensor that addresses the challenge of sensing, timing and quantifying low-light signals down to the single-photon level. Traditionally the province of the Photomultiplier Tube (PMT), the Silicon Photomultiplier now offers a highly attractive alternative that combines the low-light detection capabilities of the PMT while offering all the benefits of a solid-state sensor. The SiPM features low-voltage operation, insensitivity to magnetic fields, mechanical robustness and excellent uniformity of response. Due to these traits, the SensL SiPM has rapidly gained a proven performance in the fields of medical imaging, hazard and threat detection, biophotonics, high energy physics and LiDAR.

This document provides an introduction to SiPM sensors, explaining the working principle and primary performance parameters.

Contents

1. Photon Detection with SPAD and SiPM	2
1.1. Photon Absorption in Silicon	2
1.2. Silicon as a Photodiode.....	2
1.3. The Geiger Mode in Single Photon Avalanche Diodes (SPAD).....	2
1.4. The Silicon Photomultiplier	3
1.5. SensL's Fast Output	4
1.6. Pulse Shape.....	4
1.7. Fill Factor.....	5
2. Silicon Photomultiplier Performance Parameters	7
2.1. Breakdown Voltage and Overvoltage	7
2.2. Gain	8
2.3. Photon Detection Efficiency and Responsivity.....	8
2.4. Dark Count Rate	10
2.5. Optical Crosstalk	11
2.6. Afterpulsing	12
2.7. Dynamic Range and Linearity	12
2.8. Temperature Dependency	13
3. Other Useful Information	14
3.1. Diode Structure	14
3.2. Direct Detection of Radiation with the SiPM.....	14
4. Comparison with Other Sensor Technologies	15
5. References	16
6. Further Information	16

1. Photon Detection with SPAD and SiPM

1.1. Photon Absorption in Silicon

When a photon travels through silicon, it may be absorbed and transfer energy to a bound electron. This absorbed energy causes the electron to move from the valence band into the conduction band, creating an electron-hole pair. The absorption depth of a photon in silicon depends on its energy (or wavelength) and is shown in Figure 1. Silicon efficiently absorbs a wide range of wavelengths of light within a depth of a few tens of microns and so is well-suited as a photodetector material. As the photon absorption is wavelength dependent, it follows that the resulting photon detection efficiency of a silicon photosensor will also be wavelength dependent.

1.2. Silicon as a Photodiode

A photodiode is formed by a silicon p-n junction that creates a depletion region that is free of mobile charge carriers. When a photon is absorbed in silicon it will create an electron-hole pair. Applying a reverse bias to a photodiode sets up an electric field across the depletion region that will cause these charge carriers to be accelerated towards the anode (holes), or cathode (electrons). Therefore an absorbed photon will result in a net flow of current in a reverse-biased photodiode.

1.3. The Geiger Mode in Single Photon Avalanche Diodes (SPAD)

When a sufficiently high electric field ($> 5 \times 10^5$ V/cm) is generated within the depletion region of the silicon (achieved by the sensor design and application of a recommended bias), a charge carrier created there will be accelerated to a point where it carries sufficient kinetic energy to create secondary charge pairs through a process called impact ionization. In this way, a single absorbed photon can trigger a self-perpetuating ionization cascade that will spread throughout the silicon volume subjected to the electric field. The silicon will break down and become conductive, effectively amplifying the original electron-hole pair into a macroscopic current flow. This process is called Geiger discharge, in analogy to the ionization discharge observed in a Geiger-Müller tube.

Photon Absorption in Silicon

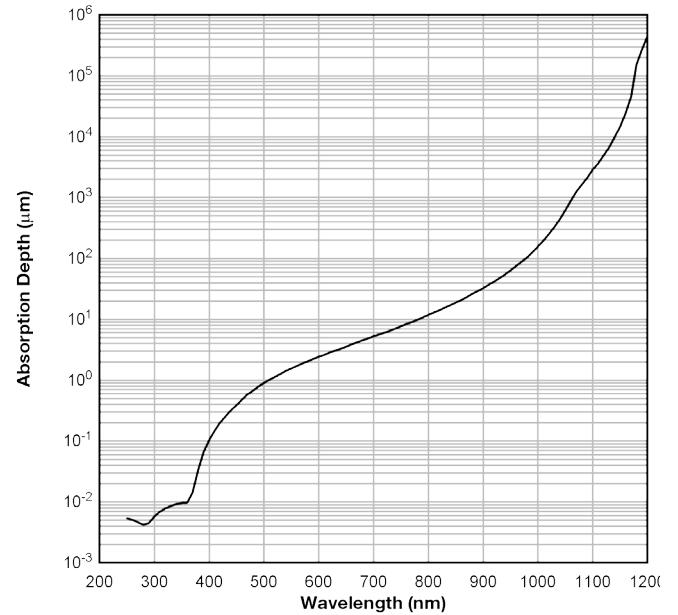


Figure 1, The photon absorption depth is the depth at which 1-1/e of the photons have been absorbed

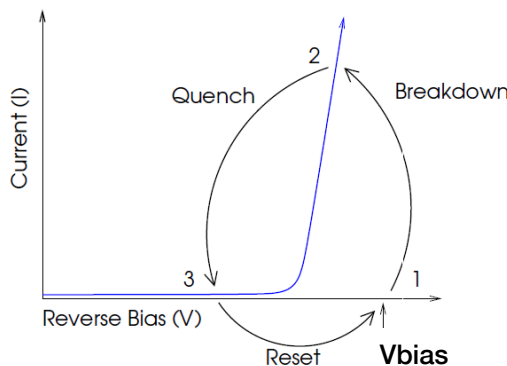


Figure 2, Breakdown, quench and reset cycle of a SPAD working in Geiger mode.

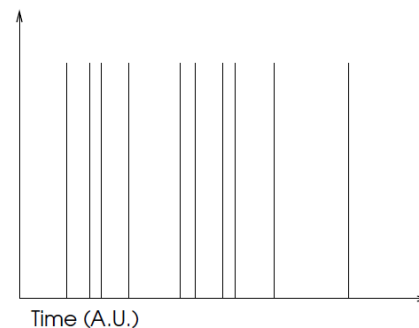


Figure 3, "digital" pulse output from a single SPAD working in Geiger mode.

A photodiode operated in Geiger mode employs this mechanism of breakdown to achieve a high gain and is referred to as a SPAD (Single Photon Avalanche Diode). The application of a reverse bias beyond its nominal breakdown voltage creates the necessary high-field gradients across the junction. Once a current is flowing it should then be stopped or ‘quenched’. Passive quenching (i.e. no active circuitry), is achieved through the use of a series resistor R_Q which limits the current drawn by the diode during breakdown. This lowers the reverse voltage seen by the diode to a value below its breakdown voltage, thus halting the avalanche. The diode then recharges back to the bias voltage, and is available to detect subsequent photons. This cycle of breakdown, avalanche, quench and recharge of the bias to a value above the breakdown voltage, is illustrated in Figure 2.

In this way, a single SPAD sensor operated in Geiger-mode functions as a photon-triggered switch, in either an ‘on’ or ‘off’ state. This results in a binary output such as illustrated in Figure 3. Regardless of the number of photons absorbed within a diode at the same time, it will produce a signal no different to that of a single photon. Proportional information on the magnitude of an instantaneous photon flux is not available.

1.4. The Silicon Photomultiplier

To overcome this lack of proportionality, the Silicon Photomultiplier (SiPM) integrates a dense array of small, independent SPAD sensors, each with its own quenching resistor. Each independently operating unit of SPAD and quench resistor is referred to as a “microcell”. When a microcell in the SiPM fires in response to an absorbed photon, a Geiger avalanche is initiated causing a photocurrent to flow through the microcell. This results in a voltage drop across the quench resistor, which in turn reduces the bias across the diode to a value below the breakdown, thus quenching the photocurrent and preventing further Geiger-mode avalanches from occurring. Once the photocurrent has been quenched, the voltage across the diode recharges to the nominal bias value. The time it takes for the microcell to recharge to the full operating voltage is called the recovery time. It is important to note that the Geiger avalanche will be confined to the single microcell it was initiated in. During the avalanche process, all other microcells will remain fully charged and ready to detect photons.

A typical SiPM has microcell densities of between 100 and several 1000 per mm^2 , depending upon the size of the microcell. A simplified electric circuit to illustrate the concept is shown in Figure 4 and a close-up image of a portion of the surface of the

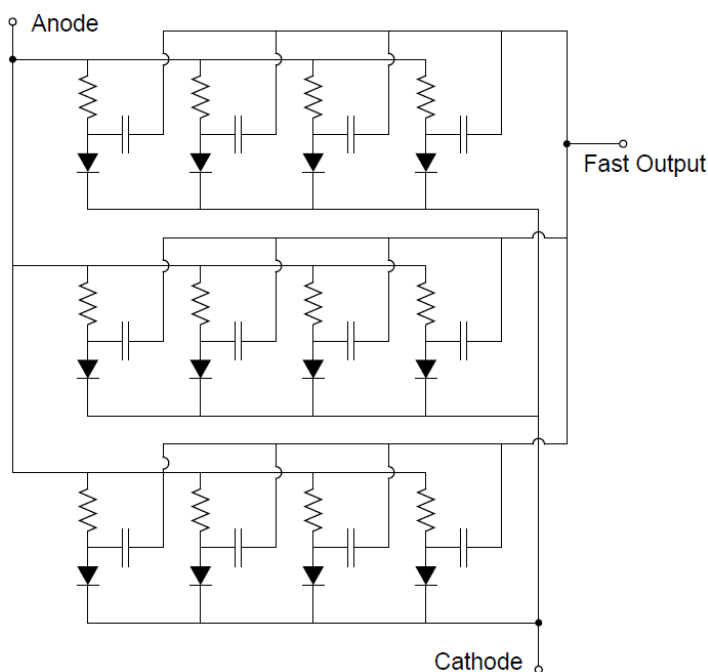


Figure 4, An SiPM consists of an array of microcells (photodiode plus quench resistor) with summed output. The fast output is discussed in section 1.5.

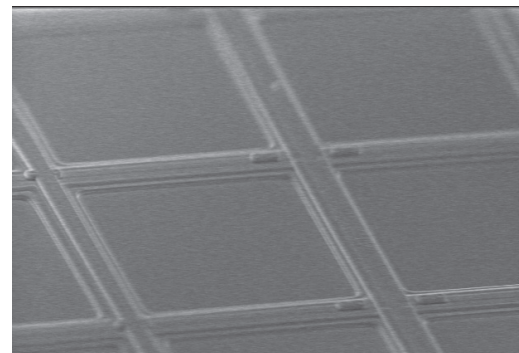


Figure 5, Image showing the microcell structure of the SiPM surface

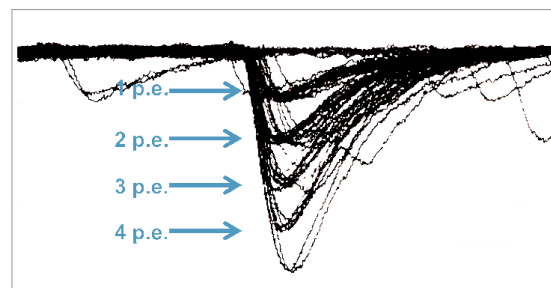


Figure 6, Oscilloscope shot showing the discrete nature of the SiPM output when illuminated by brief pulses of low-level light.

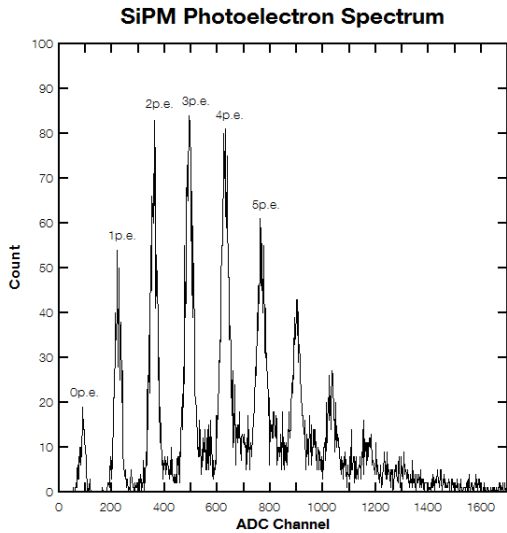


Figure 7, Photoelectron spectrum of the SiPM, achieved using brief, low-level light pulses, such as those from Fig. 6.

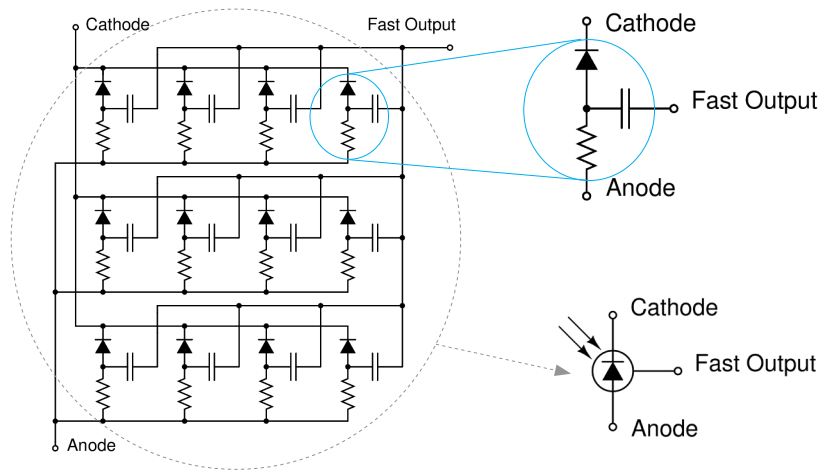


Figure 8, Simplified circuit schematic of the SensL SiPM (left) showing each microcell which is composed of the SPAD, quench resistor and fast output capacitor (top right). The SensL SiPM component symbol is shown (lower right).

SiPM is shown in Figure 5. Each microcell detects photons identically and independently. The sum of the photocurrents from each of these individual microcells combines to form a quasi-analog output, and is thus capable of giving information on the magnitude of an instantaneous photon flux. The response to low-level light pulses is shown in Figure 6, and a charge spectrum of these pulses is shown in Figure 7.

1.5. SensL's Fast Output

SensL has developed a unique modification to the standard Silicon Photomultiplier structure that results in a third terminal (in addition to the anode and cathode) carrying an ultra-fast output signal. The microcell structure schematic in Figure 8, shows how each microcell has a capacitively coupled output. This fast output signal is the derivative of the internal fast switching of the microcell in response to the detection of a single photon. The fast output, like the anode-cathode output, is formed from the sum of all microcells, as shown in Figure 8, and so proportional information on the magnitude of the photon flux can be obtained, in addition to the timing information. A typical fast output pulse is shown in Figure 9. This signal can be used to make ultra-fast timing measurements, using the ability to clearly distinguish the arrival time of the first photon in the pulse, and also allow higher count rates or the capability for second photon timing. In addition to fast timing, the fast output also has considerably lower capacitance which can be beneficial when designing readout systems for the sensor. The fast output from a 1mm sensor has a capacitance of ~1pF, whereas, reading out from the anode or cathode would have a capacitance of ~100pF.

1.6. Pulse Shape

A typical SiPM anode-cathode output pulse is shown in Figure 10. The rise time of the SiPM is determined by the rise time of the avalanche formation and the variation in the transit times of signals arriving from different points on the sensor's active area. Minimizing this transit time spread by careful design of the tracking can improve the rise time. In addition, the rise time is affected by the output impedance of the sensor and the package.

The recovery time of the sensor, or decay time of the pulse, is determined by the microcell recharge time constant, which is given by:

$$\tau_{RC} = C_d(R_q + R_s \cdot N)$$

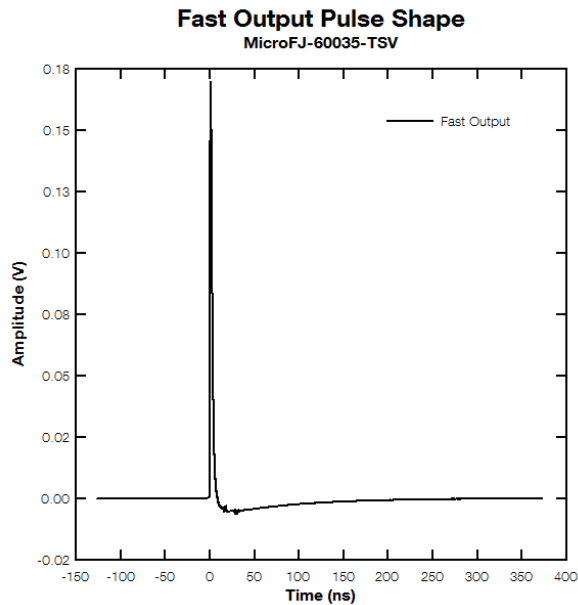


Figure 9, The fast output pulse from a 6mm sensor. The FWHM of the fast output allows the sensor to resolve high-repetition, fast pulses.

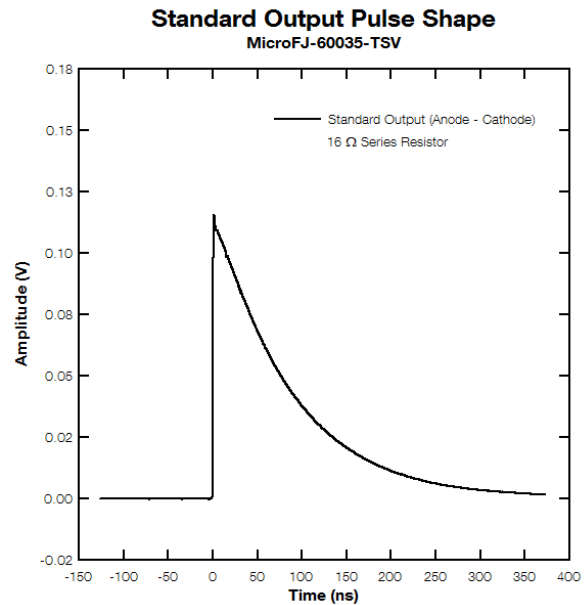


Figure 10, Output pulse read out from the anode-cathode, showing the recovery time of the microcell.

where C_d is the effective capacitance of the microcell, R_q the value of the microcell quench resistor, N is the total number of microcells in the sensor and R_s is any resistance in series with the sensor (e.g. sense resistance, signal tracks on the sensor).

Since the capacitance of the microcell will depend upon its area, the reset time will vary for different microcell sizes, with a $50\mu\text{m}$ microcell SiPM having a significantly longer reset time than a $10\mu\text{m}$ microcell SiPM.

It is important to note that the microcell can still fire during the recovery time before the overvoltage has recovered to its nominal value, but the gain will be reduced in proportion to the reduced overvoltage.

The sensor output is a photocurrent, and the total charge Q generated from an event is given by,

$$Q = N_{\text{fired}} \cdot G \cdot q$$

where N_{fired} is the number of fired microcells, G is the gain (discussed in section 2.2) and q is the electron charge. The total charge is also equal to the integral of the photocurrent pulse.

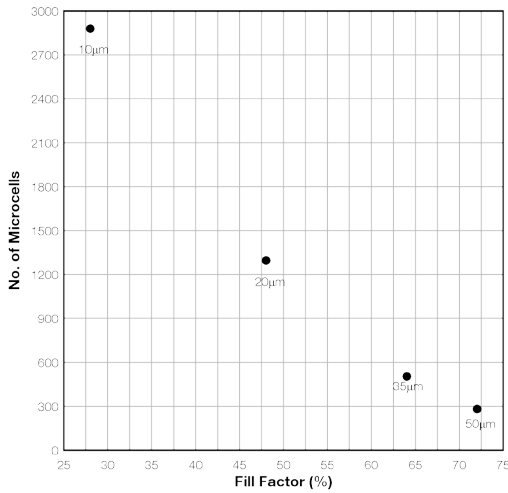
1.7. Fill Factor

The fill factor refers to the percentage of the SiPM sensor surface area that is sensitive to light. Due to the structure of the SiPM, each microcell needs to be separated from its neighbor for optical and electrical isolation purposes. In addition, some surface area is required for the quench resistor and signal tracks. All of these considerations result in a 'dead space' around the microcell. The separation between microcells and the space required for the quench resistor and tracking is more or less constant, regardless of the microcell size. Therefore, larger microcells result in a higher percentage of active surface area (active area/total area).

A higher fill factor (larger microcells) results in higher PDE and gain, but also in higher capacitances, longer recovery times and lower dynamic range.

A lower fill factor (smaller microcells) results in lower PDE and gain, but also in lower capacitances, shorter recovery times and higher dynamic range.

Microcell Number vs Fill Factor for Different Microcell Sizes
MicroFC-100XX-SMT



The trade off between fill factor and the typical number of microcells in a 1mm sensor is shown in Figure 11. The factors involved in this trade off will be discussed in more detail in the following sections. Specific values for these parameters are always in the SensL data-sheets on our website.

Figure 11, Typical fill factors and microcell numbers for a 1mm sensor from the C-Series product family.

2. Silicon Photomultiplier Performance Parameters

Users of SiPM sensors will typically need to have an understanding of the following parameters: breakdown voltage and overvoltage, gain, PDE, dark count rate (noise), optical crosstalk, afterpulsing and temperature dependency. The following sections define these parameters, and describe how they are measured. All plots used here are typical and for reference only. Please refer to the current datasheets on the [website](#) for the most up-to-date information on all of the parameters discussed here.

2.1. Breakdown Voltage and Overvoltage

The breakdown voltage (V_{br}) is the bias point at which the electric field strength generated in the depletion region is sufficient to create a Geiger discharge. The V_{br} point is clearly identified on a current versus voltage plot by the sudden increase in current, as in Figure 12. The precise value of the V_{br} is determined as the value of the voltage intercept of a straight line fit to a plot of \sqrt{I} vs V , where I is the dark current and V is the voltage, as shown in Figure 13.

SiPM sensors are operated at a bias point that is typically 10% - 25% higher than the V_{br} . The difference between the V_{br} and the bias point is referred to as the 'overvoltage' (ΔV). Both the V_{br} and the recommended ΔV range are given in the SensL product datasheets. These values allow the user to calculate the V_{bias} to apply.

$$V_{bias} = V_{br} + \Delta V$$

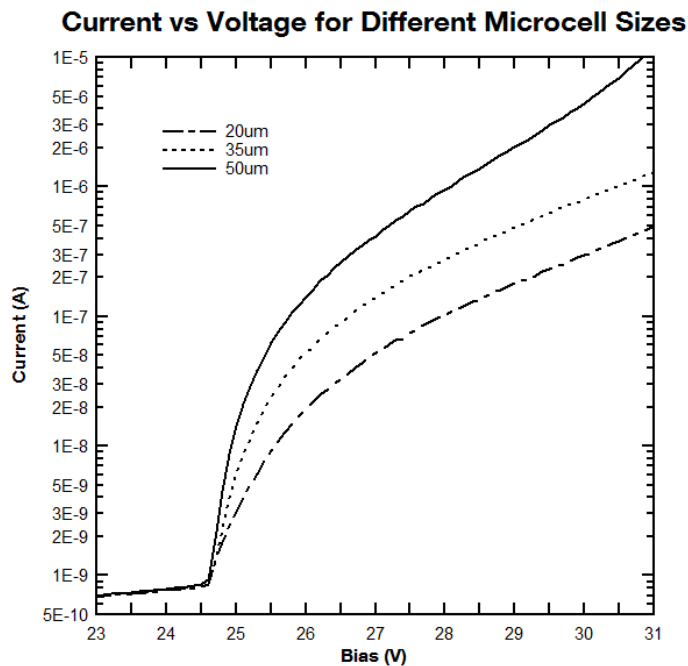


Figure 12, Dark current vs Voltage plots for 3mm sensors with 20um, 35um, and 50um microcells.

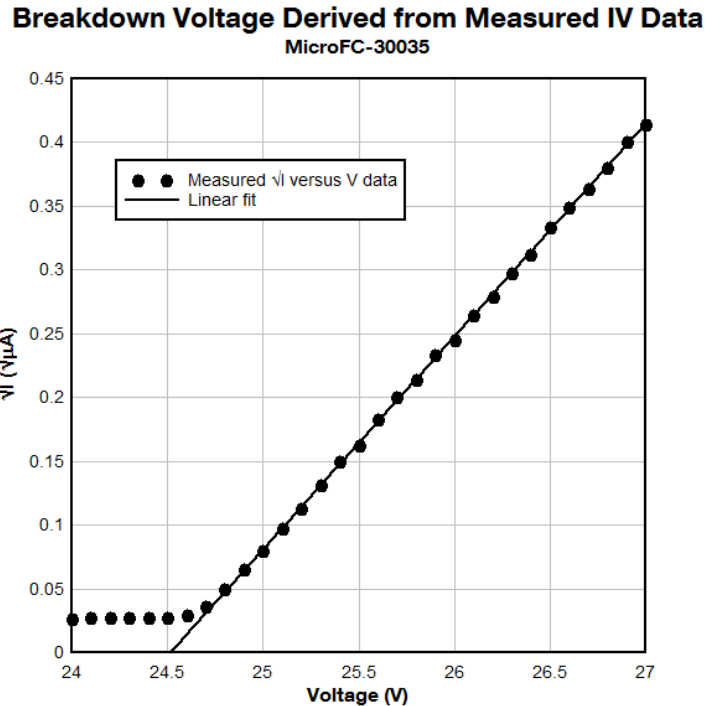


Figure 13, The breakdown voltage is determined from the intercept of a linear fit to the plot of \sqrt{I} vs V .

2.2. Gain

The gain of an SiPM sensor is defined as the amount of charge created for each detected photon, and is a function of overvoltage and microcell size, as shown in Figure 14.

Each microcell in the SiPM generates a highly uniform and quantized amount of charge every time an avalanche is generated by an absorbed photon in the active volume. The gain of a microcell (and hence the sensor) is then defined as the ratio of the charge from an activated microcell to the charge on an electron. The gain can be calculated from the overvoltage ΔV , the microcell capacitance C , and the electron charge, q .

$$G = \frac{C \cdot \Delta V}{q}$$

The unique way in which the SiPM operates can be used to accurately measure the gain. Each detected photon results in a highly quantized output pulse, as was shown in Figure 6. If the charge from each pulse is integrated and a charge spectrum is formed, the peaks due to successive numbers of detected photons will be clearly visible. Such a spectrum was shown in Figure 7. The separation between each pair of adjacent peaks (in pC) is constant and corresponds to the charge generated from a single fired microcell. This can therefore be used to accurately calculate the gain, using the equation above.

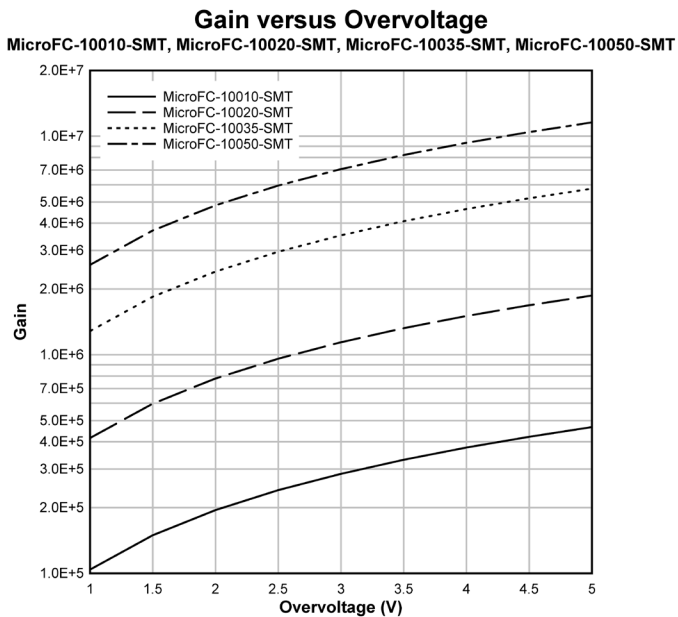


Figure 14, Gain as a function of over-voltage for different microcell size SiPMs (10um, 20um, 35um, and 50um)

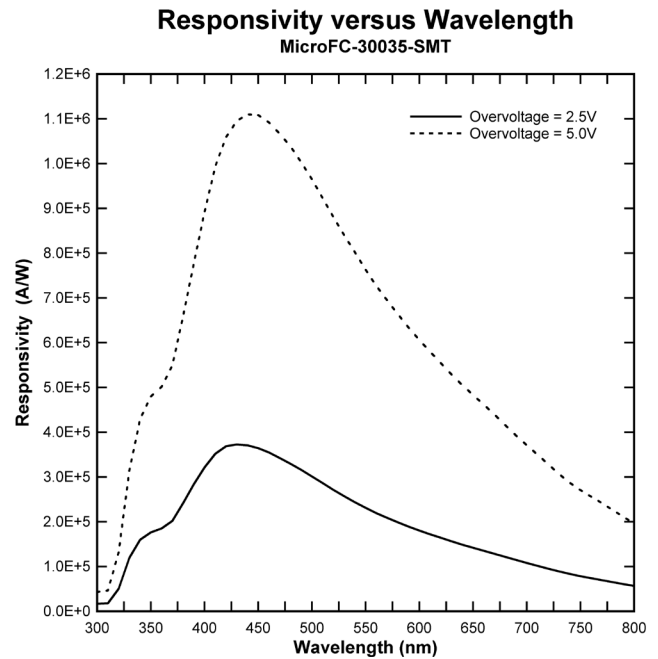


Figure 15, Responsivity as a function of wavelength for a 3mm, 35um microcell SiPM, at +2.5V and +5V overvoltage.

2.3. Photon Detection Efficiency and Responsivity

The photon detection efficiency (PDE) is a measure of the sensitivity of an SiPM and is a function of wavelength of the incident light, the applied overvoltage and microcell fill factor.

The PDE differs slightly from the quantum efficiency (QE) that is quoted for a PMT or APD, due to the microcell structure of the sensor. The PDE is the statistical probability that an incident photon interacts with a microcell to produce an avalanche, and is defined as:

$$PDE(\lambda, V) = \eta(\lambda) \cdot \epsilon(V) \cdot F$$

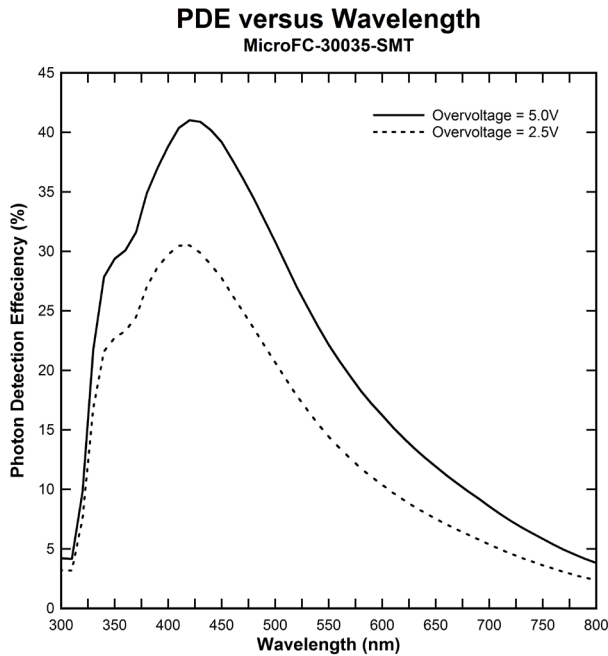


Figure 16, PDE as a function of wavelength for different overvoltages.

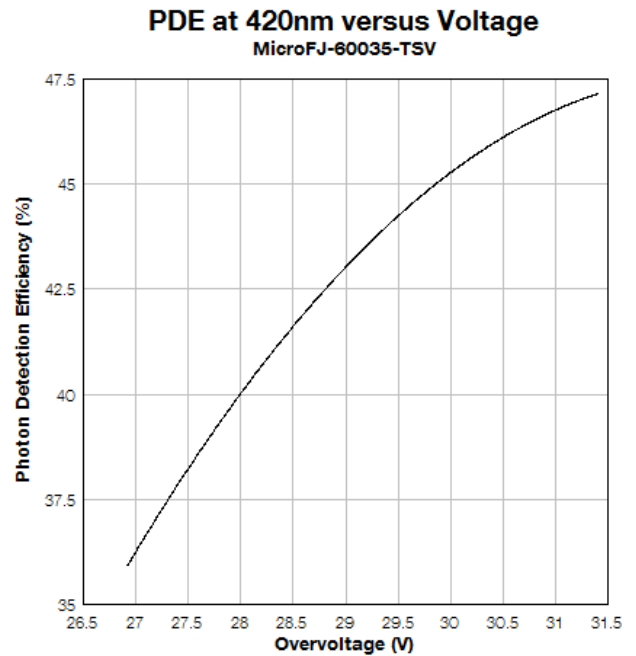


Figure 17, PDE as a function of overvoltage for a 6mm, 35um microcell SiPM

where $\eta(\lambda)$ is the quantum efficiency of silicon, $\epsilon(V)$ is the avalanche initiation probability and F is the fill factor of the device. The quantum efficiency is a measure of the likelihood of an incident photon creating an electron-hole pair in the sensitive volume of the sensor. The avalanche initiation probability takes into account the fact that not all charge carriers in the active volume will go on to initiate an avalanche. The fill factor is the ratio of active to inactive area on the SiPM, and is a result of the deadspace between the microcells and therefore depends upon the microcell size.

The PDE is commonly calculated from the responsivity of the sensor. The responsivity is defined as the average photocurrent produced per unit optical power and is given by

$$R = \frac{I_p}{P_{op}}$$

where I_p is the measured photocurrent and P_{op} is the incident optical power at a particular wavelength over the sensor area. The responsivity is typically expressed in units of Amps per Watt (A/W). Figure 15 shows a typical plot of the measured SiPM responsivity. When measuring the responsivity, low intensity light pulses should be used to ensure that the sensor is not saturated and care should be taken to have an accurate reference sensor. It should be noted that the measured responsivity will include contributions from optical crosstalk and afterpulsing (see sections 2.5 and 2.6 respectively).

The PDE can be determined from the responsivity R using the relation,

$$PDE = \frac{R \cdot h \cdot c}{\lambda \cdot G \cdot e \cdot (1 + P_{AP}) \cdot (1 + P_{XT})} \cdot 100\%$$

where h is the Planck constant, c is the speed of light, λ is the wavelength of the incident light, G is the gain, and e is the elementary charge. P_{AP} and P_{XT} are the afterpulsing and crosstalk probabilities that are measured separately and are discussed in sections 2.5 and 2.6 of this document respectively. More information on the measurement of PDE can be found in [1]. A typical PDE versus wavelength plot is shown in Figure 16. The PDE plot is used to define the peak wavelength (λ_p) and the wavelength range. A plot of the PDE at the peak wavelength versus overvoltage is shown in Figure 17.

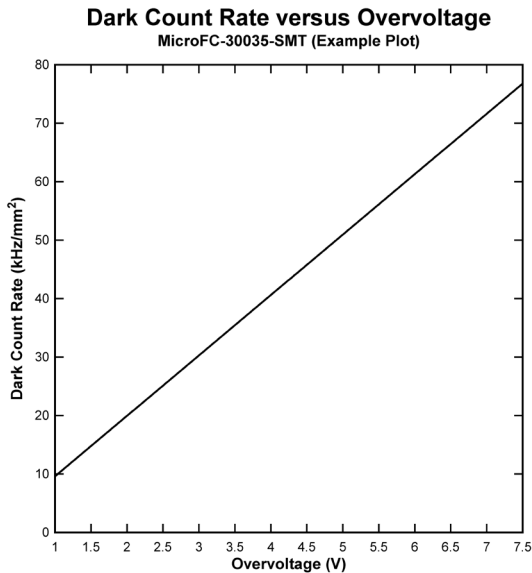


Figure 18, Dark count rate as a function of overvoltage for a 3mm, 35um microcell SiPM.

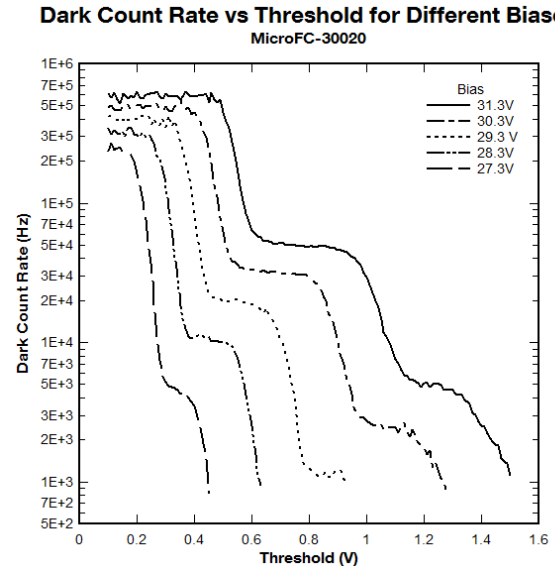


Figure 19, DCR as a function of threshold for different biases.

2.4. Dark Count Rate

The main source of noise in an SiPM is the dark count rate (DCR), which is primarily due to thermal electrons generated in the active volume. The DCR is a function of active area, overvoltage and temperature.

Each dark count is a result of a thermally generated electron that initiates an avalanche in the high field region. The signals resulting from the breakdown of the microcell, due to either photon-generated or thermally-generated electrons, are identical. Therefore, thermally generated electrons form a source of noise at the single photon level. If a threshold can be set above the single photon level then false triggers from the noise can be significantly reduced. However, the dark counts will contribute to the measured signal.

Since the dark count is comprised of a series of pulses, its magnitude is quoted as a pulse rate (kHz), or pulse rate per unit area (kHz/mm²). For continuous or current integration measurements, it is sometimes more convenient to consider the contribution as a 'dark current' which is also quoted on the SensL datasheets.

The DCR can be measured with a simple counting system, setting a threshold set at the half-photon level. The DCR increases with increasing bias as shown in Figure 18, creating an inherent trade-off between increasing PDE and DCR. The DCR also increases with increasing temperature and linearly with the active area, so a 3mm sensor will typically have 9 times the DCR of a 1mm sensor.

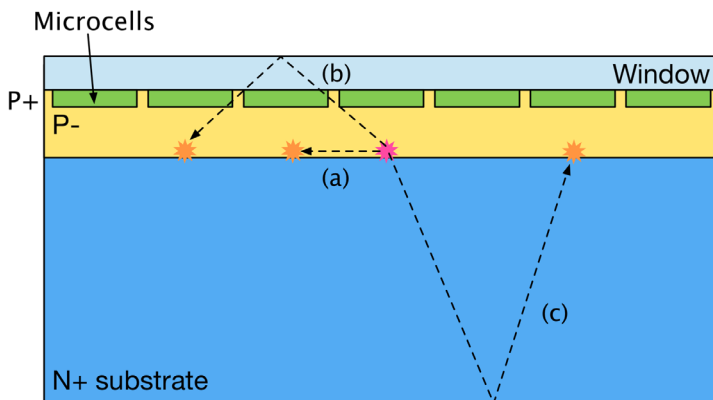


Figure 20, An illustration of the various ways in which secondary photons can travel to neighboring microcells to cause optical crosstalk.

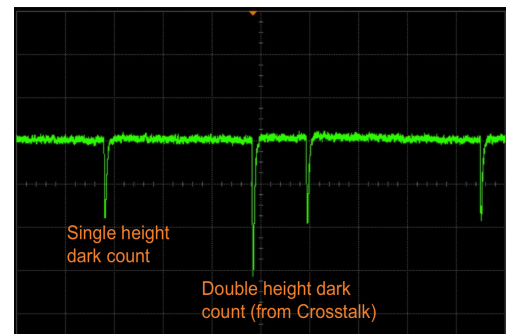


Figure 21, Oscilloscope shot showing dark counts

2.5. Optical Crosstalk

An additional component of SiPM noise is that of optical crosstalk between microcells. Optical crosstalk is a function of overvoltage and is also affected by the fill factor of a sensor.

During avalanche, accelerated carriers in the high field region will emit photons that can initiate a secondary avalanche in a neighboring microcell. These secondary photons tend to be in the near infrared (NIR) region and can travel substantial distances through the silicon. Typically 2×10^{-5} NIR photons are emitted per electron crossing the junction. As shown in Figure 20, the secondary photons can travel to neighboring microcells via a number of routes: a) directly to a neighboring microcell, b) reflected from the window material on the top of the sensor (usually epoxy or glass), or c) reflected from the bottom of the silicon substrate.

The crosstalk is defined as the probability that an avalanching microcell will cause an avalanche in a second microcell. The process happens instantaneously and as a consequence, single incident photons may occasionally generate signals equivalent to 2 or 3 photons, or even higher. This effect can be seen in Figure 21, which shows the output of a sensor in the dark, and so all of the signal pulses are due to dark counts. The central dark count pulse shown in Figure 21 has a pulse height that is double that of the other dark counts that are at the single photon level, and so will be due to a crosstalk event. The optical crosstalk can be estimated by measuring the ratio of the count rate at the second photon level to the count rate at the single photon level. Figure 19 shows the result of plotting the DCR as a function of threshold position, which produces a step-like plot. The flat regions of the curve correspond to the frequency of dark counts at the single, double, triple photon level etc. Crucially, this plot shows that with a threshold level set at the level of a ~ 3 photons, the dark count trigger rate will be negligible.

Figure 22 shows the crosstalk increasing with overvoltage, which is due to the increased number of carriers crossing the junction due to higher gain. There is an inherent trade off between PDE (maximized using a high overvoltage) and cross talk (minimized using a lower overvoltage). Therefore, plots of the type in Figure 23 can be useful. The subject of optical crosstalk in SPAD arrays is discussed in detail in by Rech et al. [2] and crosstalk measurement in SiPM sensors is also discussed by Eckert et al. [1].

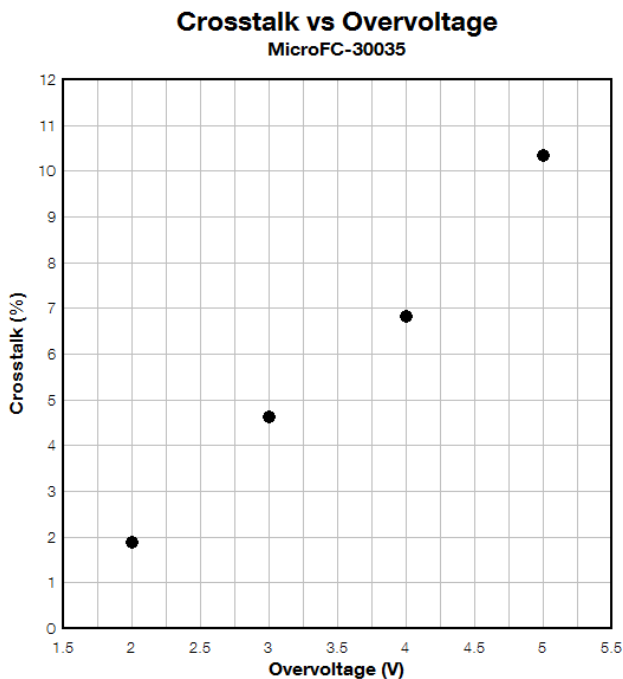


Figure 22, Crosstalk vs Overvoltage for 3mm SiPM with 35um microcells

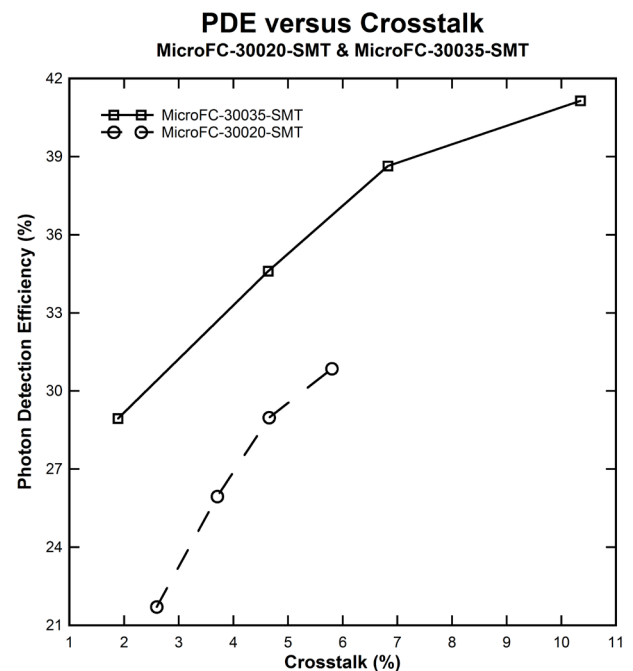


Figure 23, PDE vs Crosstalk for 3mm SiPM with 20um and 35um microcells

2.6. Afterpulsing

During breakdown, carriers can become trapped in defects in the silicon. After a delay of up to several ns, the trapped carriers are released, potentially initiating an avalanche and creating an afterpulse in the same microcell. Afterpulses with short delay that occur during the recovery time of the microcell tend to have negligible impact as the microcell is not fully charged. However, longer delay afterpulses can impact measurements with the SiPM if the rate is high. SensL devices have particularly low afterpulsing due to process defect reduction. The afterpulse probability is determined by measuring the statistical distribution of consecutive pairs of dark counts, when triggered at one half of the single photoelectron amplitude. Afterpulse probability increases with overvoltage (due to increased avalanche initiation probability). Eckert [1] discusses afterpulsing in more detail including its measurement in SiPM sensors.

2.7. Dynamic Range and Linearity

The dynamic range of a given SiPM sensor can be defined as the optical signal range over which the sensor provides a useful output.

The dynamic range is a function of the total number of microcells, the overvoltage used, and the wavelength of the incident photons. The relationship between the number of incident photons (N_{ph}) and the number of fired microcells (N_{fired}) is given as,

$$N_{fired}(M, V, \lambda) = M \left(1 - \exp \left(- \frac{PDE(V, \lambda) \cdot N_{ph}}{M} \right) \right)$$

where M is total number of microcells, λ is the wavelength of the incident photons, V is the overvoltage and PDE is the photon detection efficiency. An example plot generated using this equation for 1mm, 3mm and 6mm sensors is shown in Figure 24. It can be seen that the sensor has a linear response at lower photon fluxes, but as the number of incident photons increases the sensor output becomes non-linear. This deviation from linearity is linked to the total number of microcells in the sensor: more microcells result in a larger dynamic range. Therefore, for a given sensor size, smaller microcells will result in a larger dynamic range than larger microcells. A general rule of thumb to maintain an approximately linear response, is to match the maximum expected power to $\sim 70\%$ of the SiPM range, which is more clearly seen in Figure 25.

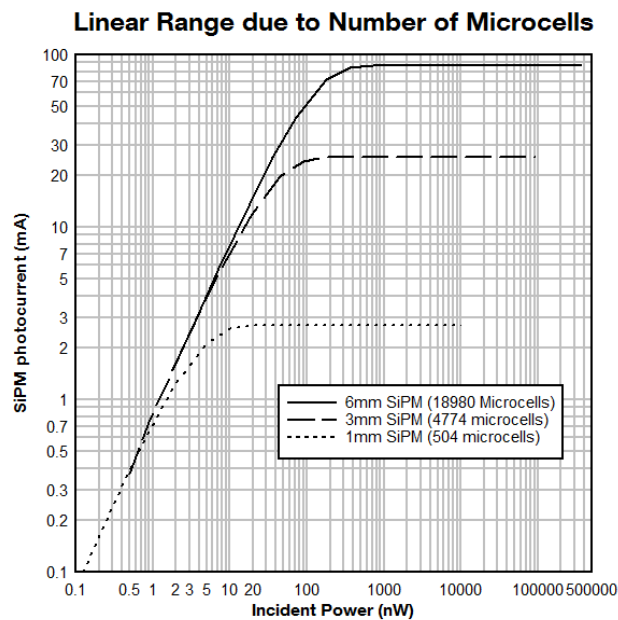


Figure 24, The SiPM photocurrent as a function of incident power on a log-log scale. The SiPM maintains a linear response at higher levels of incident light when there are more microcells.

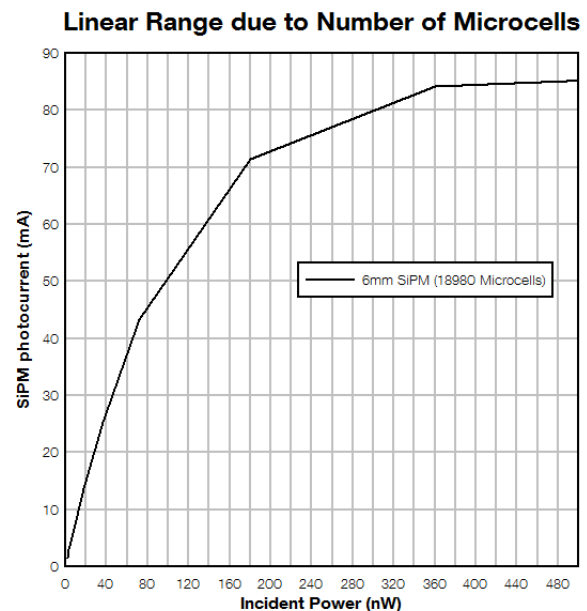


Figure 25, The SiPM photocurrent as a function of incident power for a 6mm sensor on a linear scale. As a rule of thumb, linearity drops off at about 70% of the full SiPM range.

2.8. Temperature Dependency

The primary effects of temperature change on the SiPM are a change in the breakdown voltage and the dark count rate.

The breakdown voltage changes linearly as a function of temperature, as shown in Figure 26. The effect for SensL SiPM is small (21.5mV/°C) and so in many applications compensation for this change may not be required. However, if large temperature fluctuations are experienced and not compensated for, it will result in changes in the effective overvoltage, which in turn affects many of the SiPMs performance characteristics.

For stable operation in the presence of significant temperature fluctuations, either bias compensation or thermal regulation should be considered. Bias compensation is the simpler of the two methods. The bias is automatically adjusted in response to a change in the temperature to ensure a constant overvoltage is maintained.

If a constant overvoltage is maintained, most parameters, such as gain, PDE and timing, will remain the same as at room temperature. However, regardless of constant overvoltage, the DCR will be altered by a change in temperature, as shown in Figure 27, due to a change in the generation rate of thermal electrons in the sensitive volume.

An increase in temperature will increase the dark count rate, and the converse is also true: for every 10°C reduction in device temperature, there is a 50% decrease in the dark count rate. Therefore actively cooling an SiPM will significantly reduce the DCR.

Operating Voltage Variation versus Temperature

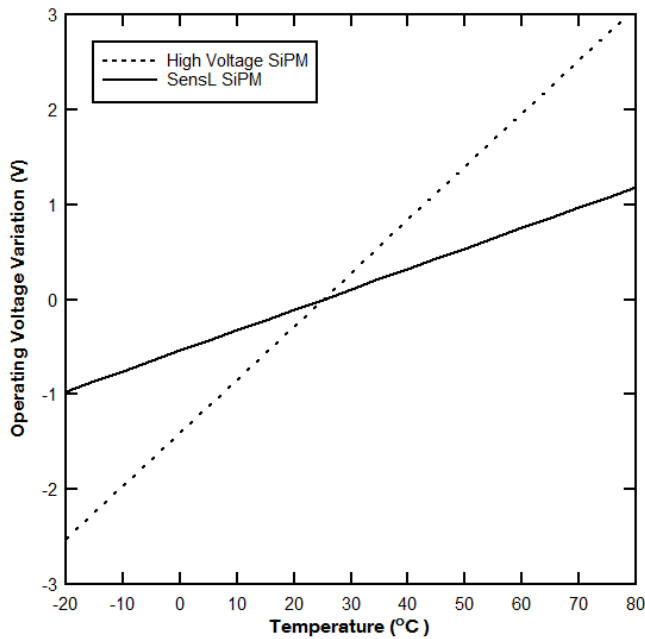


Figure 26, The impact of temperature change on the operating voltage, for a SensL sensor and an SiPM with a higher breakdown voltage.

DCR versus Temperature and Bias
MicroFC-30035

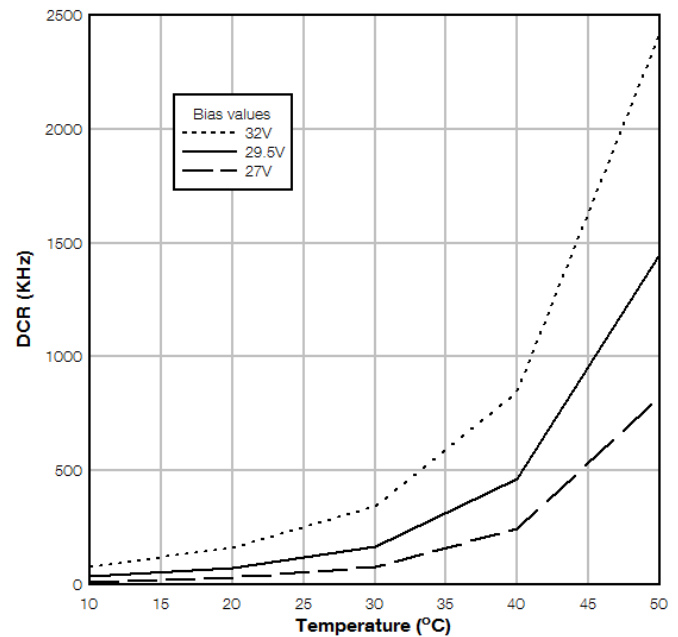


Figure 27, The impact of temperature change on dark count rate (DCR) for different bias values.

3. Other Useful Information

3.1. Diode Structure

The diode can be fabricated as either a P-on-N type or N-on-P type, as illustrated in Figure 28. Since electrons have a higher probability than holes of initiating an avalanche, better efficiency can be achieved when the initial photon interacts in the p-type layer. This maximizes the flow of electrons through the high-field avalanche region. Therefore, to maximise sensitivity to shorter wavelength (blue) photons, a P-on-N structure is more efficient, while an N-on-P structure can give better sensitivity to longer wavelength photons (green-red).

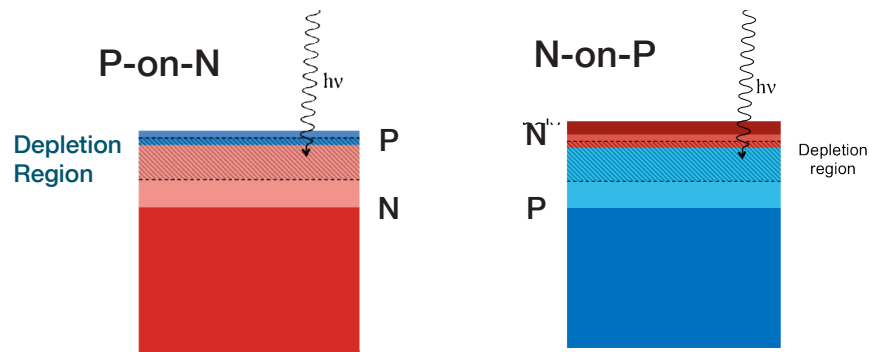


Figure 28, Different diode structures. P-on-N gives best sensitivity to shorter wavelengths and N-on-P for longer wavelengths.

3.2. Direct Detection of Radiation with the SiPM

It is possible to use some silicon sensors, such as the PIN or APD, for the direct detection of radiation such as X-rays or gamma rays. This is because the photon produces ionization in the sensitive volume, which is then translated into a proportional output by the sensor. However, direct detection of radiation with the SiPM is not generally possible. This is for two reasons: The sensitive volume in the SiPM is of the order of a few microns deep, which provides very poor stopping efficiency for all but the lowest of X-ray energies. Secondly, the ionization produced by the radiation would not yield a proportional response. Assuming all of the ionization occurs in one microcell, then the signal of '1' is produced, regardless of the amount of ionization actually deposited. Therefore, no proportional (energy) information could be recorded about the incident radiation.

4. Comparison with Other Sensor Technologies



Figure 29, A typical PMT

Low-light photon sensors constitute the enabling technology for a diverse and rapidly growing range of applications: nuclear medicine, hazard and threat detection, high energy physics, biophotonics, and LiDAR all require sensors that quantify and/or time-stamp light signals with anywhere from one to several thousands of photons per event. The ideal photosensor provides a response proportional to the incident photon flux and incorporates an internal gain mechanism, yielding signals of sufficient magnitude as to be easily processed. It should offer sub-nanosecond response times and broad spectral sensitivity, be robust, easy to operate and only generate manageable amounts of noise or dark count rates.

To date the photomultiplier tube (PMT), a well established and widely available vacuum tube device, has been the sensor of choice for many applications. The semi-transparent photocathode deposited inside the entrance window inherently limits the QE that can be achieved, with typical PMTs having about 25% at 420nm. A gain of 1×10^6 is achieved at the cost of a high bias voltage of 1-2kV, which requires the use of costly high-voltage power supplies. PMTs are generally stable and low noise but are bulky and delicate due to their vacuum-tube structure. They can also be adversely affected by magnetic fields which will limit their suitability for some applications.

Solid state devices have many practical advantages over the PMT, and this has led to the PIN diode being used in applications where PMTs were too bulky or delicate, or where high voltages are not possible. However, PIN diodes are severely limited by their complete lack of internal gain. The Avalanche Photodiode (APD) is another technology, an extension of the simple PIN diode. Here the reverse bias is raised to a point where impact ionization allows for some internal multiplication, but is below the breakdown bias where the Geiger mode would take over. In this way, a gain of around a 100 is achieved for a bias of 100-200V. With special manufacture, it is possible for gains of several thousand to be reached using an HV bias of $>1500V$. Whilst the gain may be lower than that of a PMT, APDs have the advantage of a QE which can be $>65\%$ and are also compact, rugged and insensitive to magnetic fields. Their main drawbacks are their excess noise (associated with the stochastic APD multiplication process) and in an important trade-off: The capacitance increases with increasing device area and decreasing thickness, whereas the transit times of the charge carriers increase with increasing thickness, implying a performance trade-off between noise and timing. They are limited in size to $\sim 10mm$ diameter.

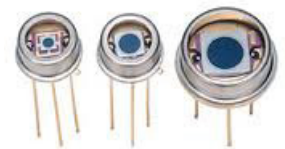


Figure 30, APD sensors

The SiPM has high gain (1×10^6) and PDE ($>50\%$) combined with the physical benefits of compactness, ruggedness and magnetic insensitivity. In addition, the SiPM achieves its high gain with very low bias voltage ($\sim 30V$) and the noise is almost entirely at the single photon level. Because of the high degree of uniformity between the microcells the SiPM is capable of discriminating the precise number of photons detected as distinct, discrete levels at the output node. The ability to measure a well resolved photoelectron spectrum is a feature of the SiPM which is generally not possible with PMTs due to the variability in the gain, or excess noise. Further technical details on SensL's full range of SiPM sensors can be found at www.sensl.com/products/

5. References

- [1] P. Eckert et al., “*Characterisation studies of silicon photomultipliers,*” Nucl. Instrum. Methods Phys. Res. A 620, 217–226 (2010).
- [2] I. Rech et al., “*Optical crosstalk in single photon avalanche diode arrays: a new complete model,*” Optics Express Vol. 16, No. 12, 8381 (2008).

6. Further Information

The SensL website contains a large amount of additional information:

Access information on our product ranges here: <http://sensl.com/products/>

A library of academic journal articles that use SensL SiPM sensors can be found here: <http://sensl.com/documentation/academic-research-library/>

A large number of technical notes and white papers can be found here: <http://sensl.com/documentation/>

The white paper “[How to Evaluate and Compare SiPM Sensors](#)” is a good follow-up document to this introduction document.